Available online at www.sciencedirect.com
SCIENCE DIRECT
Icarus 177 (2005) 297–304
ICARUS
www.elsevier.com/locate/icarus

Model constraints on the opening rates of bands on Europa

Michelle M. Stempel [1], Amy C. Barr [2], Robert T. Pappalardo [*]

Laboratory for Atmospheric and Space Physics, University of Colorado at Boulder, Campus Box 392, Boulder, CO 80309-0392, USA

Received 20 July 2004; revised 14 March 2005

Available online 5 July 2005

Abstract

A mid-ocean-ridge spreading analog is used to constrain the opening rates and brittle–ductile transition depths for two axisymmetric ridged bands on Europa. Estimates of brittle–ductile transition depth based on the morphologies of Yelland and Ino Lineae are combined with a conductive cooling model based on a mid-ocean ridge analog to estimate the opening rates and active lifetimes of the bands. This model limits local strain rates to $\sim 10^{-15}$–10^{-12} s^{-1}, opening rates to 0.2–40 mm yr^{-1}, and active lifetimes of the bands to 0.1–30 Myr. If the observed structures in the outer portions of ridged bands are indeed normal faults, the estimated range for the tensile strength of ice on Europa is 0.4–2 MPa, consistent with nonsynchronous rotation as the dominant driving mechanism for band opening.

Keywords: Europa; Geological processes; Geophysics; Satellites of Jupiter; Tectonics

1. Background: morphology of bands

Europa's surface exhibits varied morphology, including linear features with a range of widths and lengths such as troughs, double ridges, and bands (Greeley et al., 2004). Based on morphological transitions among them, it is inferred that troughs develop to form ridges, which in turn can develop into wider and more complex bands (Head et al., 1999; Prockter et al., 2002). Bands themselves are not all alike: some show subparallel or intersecting ridges, and others are relatively smooth containing fine-scale hummocks (Figueredo and Greeley, 2000, 2004; Prockter et al., 2002).

Here we concentrate on a band type described by Prockter et al. (2002) which we term *ridged bands*. Ridged bands exhibit grossly axisymmetric morphology with a narrow, linear central trough, flanked by a hummocky textured zone. Beyond the hummocky zone is a series of alternating bright and dark lineations that define subparallel ridges and troughs which are similar in their characteristics to imbricate fault blocks. Ridged bands commonly show a ridge at the sharp boundary with the surrounding terrain, suggesting exploitation of a preexisting double ridge during band formation (Prockter et al., 2002).

Stereo images of several ridged bands show raised topography relative to the surrounding ridged plains, consistent with emplacement of buoyant subsurface material, plausibly ice that is warmer and/or compositionally cleaner than its surroundings (Nimmo et al., 2003). Upwelling of viscous ice through a plane of weakness in the brittle surface layer and separation of the opposing lithospheric blocks suggests that bands are analogous to mid-ocean-ridge (MOR) spreading centers on Earth (Sullivan et al., 1998; Prockter et al., 2002).

2. Mid-ocean ridge analog model

2.1. Conceptual analog

Fig. 1 displays the ridged bands explored in this study, located at approximately 16° S, 196° W, in the antijovian

* Corresponding author. Fax: +1 303 492 6946.
E-mail address: robert.pappalardo@colorado.edu (R.T. Pappalardo).
[1] Now at: California Institute of Technology, Division of Geological and Planetary Sciences, 1200 E. California Blvd., Pasadena, CA 91125, USA.
[2] Now at: Washington University, Department of Earth and Planetary Sciences, Campus Box 1169, St. Louis, MO 63130, USA.

0019-1035/$ – see front matter
doi:10.1016/j.icarus.2005.03.025

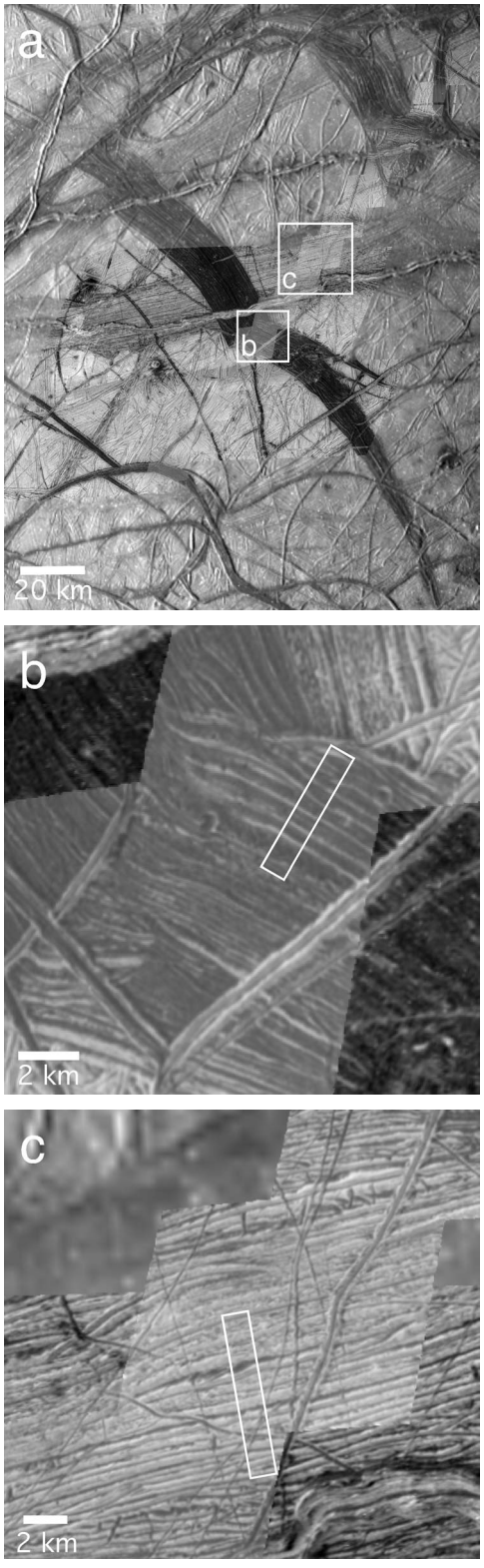

Fig. 1. (a) Yelland and Ino Lineae, located in the Argadnel Regio (the "wedges region") of Europa, intersect near 16° S, 196° W. Older gray band Ino Linea is cross-cut by the younger dark band Yelland Linea. Enlargements show (b) Yelland and (c) Ino in greater detail, from the 25 m/pixel Galileo image mosaic 12ESWEDGE_02. White rectangles on these enlargements show the areas where brightness profiles were obtained (see Fig. 3). Projection is Lambert conformal conic.

"wedges" region, Argadnel Regio. The younger dark band Yelland Linea (∼18 km at its widest) crosscuts the older gray band Ino Linea (∼20 km wide). Both display a narrow central trough, flanked by a hummocky zone, and straddled by subparallel ridges and troughs, as is characteristic of Europa's ridged bands.

Ridged bands are similar in overall morphology to some MOR spreading zones on Earth. Prockter et al. (2002) examine several europan bands, and observe a continuum of band morphologies, considered to represent various rates of spreading. Faster spreading rates are hypothesized to form smooth bands, whereas slower spreading rates might produce features more analogous to MORs on Earth, with a medial trough flanked by distinct subparallel normal faults. The observed morphologies of Yelland and Ino Lineae appear to be analogous to MORs on Earth (Fig. 2).

On Europa, as at terrestrial spreading centers, extension is expected to create axisymmetric structures. We hypothesize that the hilly appearance of the hummocky zone in Yelland and Ino Lineae is the surface expression of lithosphere too thin to permit lithostatic stress sufficient to induce normal faulting. The hummocky zone is instead postulated to be dominated by shallow tension fractures. This behavior is observed in the southwest volcanic zone of Iceland, where tension fractures in ice attain a certain maximum scale (Gudmundsson, 1987). Below this critical depth, the greater overburden stress leads to shear failure and normal faulting (cf. Suppe, 1985, p. 192).

We assume a similar transition of failure styles for Yelland and Ino Lineae. We consider the straddling lineated zone to be a region where band material has cooled appreciably, attaining a thickness greater than that necessary to transition from tension fractures to normal faults, allowing lithostatic stresses to induce imbricate block faulting. The inferred normal fault blocks of the lineated zone are aligned near-orthogonally to the band opening direction (Prockter et al., 2002).

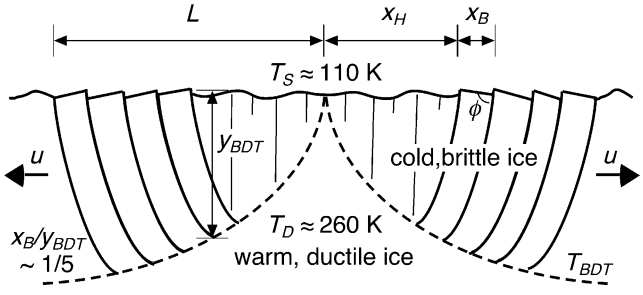

Fig. 2. Schematic illustration of the cross-section of an active band on Europa, modeled as an analog to mid-ocean-ridge spreading centers on Earth. Near-vertical tension cracks can form in the inner hummocky zone of the band. Imbricate normal faulting (potentially listric) is inferred from alternating bright and dark albedo lineations that straddle the hummocky zones of Yelland and Ino Lineae. Fault blocks of width x_B first occur at a distance x_H from the band axis, and determine the depth to the brittle–ductile transition y_{BDT} for an assumed width-to-depth ratio x_B/y_{BDT}. The brittle–ductile transition is represented by dashed curves, and the half-width of the band is L.

At terrestrial spreading zones, cooling of oceanic lithosphere creates a density gradient that pulls the relatively thin lithosphere away from the rift zone to cause MOR extension (Turcotte and Schubert, 2002). In contrast to Earth's oceanic crust, the brittle layer on Europa is assumed to be relatively thick, and may be a significant fraction of the thickness of the solid ice shell. Tension instead allows for buoyant, ductile ice to rise toward the surface, contributing to the emplacement of new icy lithospheric material.

Slow nonsynchronous rotation (Helfenstein and Parmentier, 1985; McEwen, 1986; Leith and McKinnon, 1996) and rapid diurnal tidal flexing (Greenberg et al., 1998; Hoppa et al., 1999) are the most likely sources of this tensile stress. Inferred nonsynchronous rotation of Europa's icy shell about a tidally locked interior may contribute significantly to the magnitude and direction of surface stresses, potentially providing ~0.1 MPa of stress for each degree of shell rotation, and possibly accumulating for up to tens of degrees. Diurnal stresses are limited to a maximum of ~0.1 MPa and vary in direction and magnitude throughout the satellite's 85-h orbital period (Greenberg et al., 1998).

The morphological similarities between MORs and bands on Europa motivate us to apply a simple MOR spreading model (Turcotte and Schubert, 2002) to the formation of bands (Fig. 2). The thermal structure beneath mid-ocean ridges on Earth can be modeled from the balance between cooling of the oceanic lithosphere with surface temperature T_s above a warm, semi-infinite half-space of temperature T_m. The thickness of the terrestrial oceanic lithosphere increases as a function of distance from the spreading axis, and depends on u, the half-spreading rate of the ridge. The depth to a given isotherm, such as the brittle–ductile transition (BDT) temperature (T_{BDT}), increases as the square root of distance from the spreading axis.

Applying this model to Europa, an estimate of the BDT isotherm (y_{BDT}) at the edge of the hummocky zone, where we assume that the lithosphere first becomes thick enough to fault, constrains the opening rate of the band. The BDT depth and the width of the hummocky zone are estimated through measurements of the morphology of Yelland and Ino Lineae (Table 1). We observe a fault block width x_B at a distance x_H from the central trough, and constrain the BDT depth y_{BDT} by assuming a width-to-depth ratio x_B/y_{BDT}. This depth and half-width L of the band allow inference of the spreading rate of the band and the BDT temperature (see Fig. 2).

2.2. Measurements of band morphology

Measurements of hummocky zone half-width (x_H), fault block width (x_B), and band half-width (L) are obtained across the northeast portion of Yelland Linea just below its 'dogleg' directional change, and across the southern portion of Ino Linea, just east of where it is crosscut by Yelland Linea (Fig. 1). The hummocky zone half-width and band half-width are determined from averaged data number (DN) profiles across images of the bands (Fig. 3). Six closely spaced transects from each band are horizontally aligned by using prominent features which appear in each individual profile. The average block spacing is determined by dividing the width of the lineated zone by the number of brightness peaks in the averaged profile (see Fig. 3). Results are listed in Table 1.

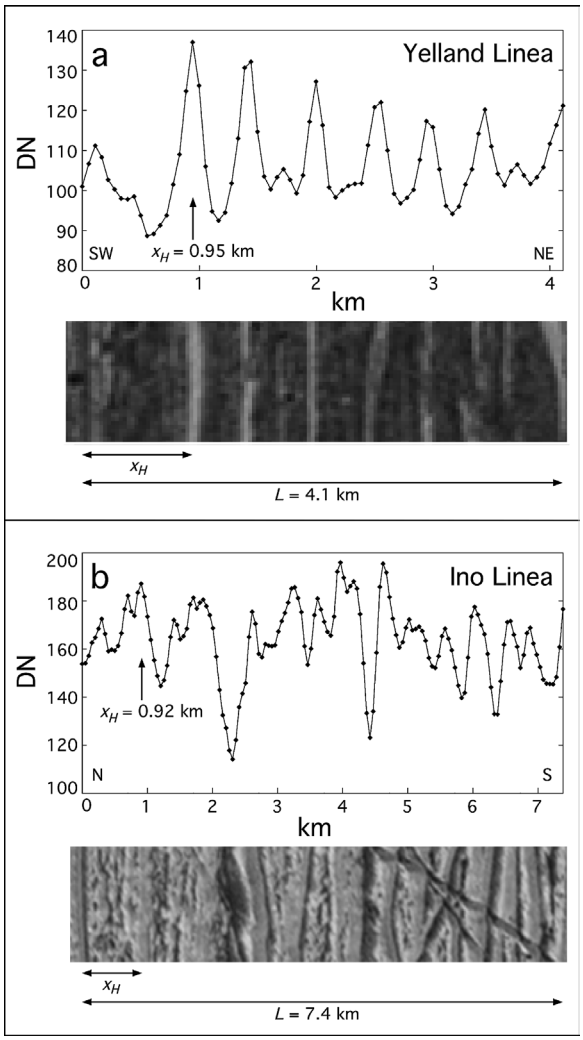

Fig. 3. Closely spaced transects across Galileo images are averaged to evaluate the typical change in brightness with distance from the axial trough of (a) Yelland Linea and (b) Ino Linea. Brightness peaks in the data number (DN) profiles correlate with observable lineations in each band, as seen by direct comparison to image segments aligned below the averaged profiles. The transition from hummocky zone to lineated region is distinct for Yelland Linea, as are its 6 brightness peaks inferred to delimit imbricate fault blocks. These characteristics are less apparent for Ino Linea, because of the gray band's lesser contrast and because other narrow lineaments cross-cut the 13 bright subparallel lineations in this band. Inferred hummocky zone width x_H and band half-width L are as indicated.

When estimating fault block width from Galileo images, we have neglected the geometric effect of fault dip (ϕ of Fig. 2), so the spacing between blocks is overestimated by a factor of $\sin(\phi)$. Faults that evolve from tension fractures are expected to have steep near-surface dips, so $\sin(\phi) \sim 1$, and

Table 1
Band dimensions

	Yelland	Ino
x_H (km)	0.95	0.92
x_B (km)	0.50	0.55
L (km)	4.1	7.4

the slight error in x_B will not significantly alter the model results.

Yelland Linea tapers to the southeast (Fig. 1). This narrow region might be expected to spread at a slower rate than where the measurements are made if material was emplaced along Yelland over a similar active lifetime. Unfortunately, a lack of high-resolution images of the tapered end of Yelland precludes rigorous testing of this assumption.

2.3. Analytical model

In the mid-ocean ridge model (Turcotte and Schubert, 2002), the half-spreading rate u is related to y_{BDT} and x_H as

$$u = \kappa x_H \left(\frac{2\mathrm{erfinv}(\frac{T_{BDT}-T_S}{T_D-T_S})}{y_{BDT}} \right)^2. \quad (1)$$

The inverse error function (erfinv) relates T_{BDT} to the surface temperature ($T_S = 110$ K) and the temperature of the underlying isothermal material (in this case, ductile ice with $T_D \approx 260$ K); κ is thermal diffusivity (1×10^{-6} m^2 s^{-1} for ice). The hummocky zone width (x_H) is taken as equivalent to the distance from the central trough to the first prominent normal fault (Fig. 3; see Table 1 for values). The depth to the BDT isotherm y_{BDT} is constrained by the measured widths of fault blocks and an assumed range in plausible fault block x_B/y_{BDT} ratio.

The brittle–ductile transition temperature beneath bands on Europa will depend on the rheology of ice, the strain rate associated with band opening, and the coefficient of internal friction relevant to the brittle lithosphere. We determine a value for T_{BDT} by equating the brittle failure strength ("Byerlee's law") for ice (Beeman et al., 1988) to the ductile flow law for ice (Goldsby and Kohlstedt, 2001). The brittle failure strength for a material is the differential stress at failure

$$\Delta\sigma = \sigma_1 - \sigma_3. \quad (2)$$

In the mid-ocean ridge analog model, the greatest compressive stress σ_1 is lithostatic, such that

$$\sigma_1 = \rho g y_{BDT} \quad (3)$$

and the least compressive stress σ_3 is horizontal, given by

$$\sigma_3 = \sigma_1 \left(\frac{\sqrt{\mu^2+1}-\mu}{\sqrt{\mu^2+1}+\mu} \right) \quad (4)$$

(Jaeger and Cook, 1979, p. 96, with cohesion of the brittle material taken to be zero). Here ρ is density of ice (assumed 920 kg m^{-3}), g is gravitational acceleration (1.3 m s^{-2} for Europa), and μ is the coefficient of internal friction. A friction coefficient $\mu = 0.65$ for cold ice is determined from laboratory experiments at low temperatures (Beeman et al., 1988). At temperatures closer to the ice melting point, $\mu = 0.1$ (Kennedy et al., 2000), which may apply along a band's axis where warm ice upwells. These two values of μ are considered as endmembers here.

The differential stress that allows for the ductile flow of ice is given by

$$\Delta\sigma = \left(\frac{\dot{\varepsilon} d^p}{A} \right)^{-n} \exp\left(\frac{Q}{nRT_{BDT}} \right), \quad (5)$$

where

$$\dot{\varepsilon} \approx \frac{u}{x_H} \quad (6)$$

is the strain rate; d is grain size of ice (here we assume endmembers of 1 mm and 1 cm); p, A, n, and Q are ice creep constants for either grain boundary sliding (GBS) or dislocation creep as determined experimentally by Goldsby and Kohlstedt (2001). For GBS, these parameters are: $p = 1.4$; $A = 6.2 \times 10^{-14}$ Pa$^{-1.8}$ d$^{1.4}$ s^{-1}; $n = 1.8$; and $Q = 49$ kJ mol^{-1}. For dislocation creep: $p = 0$; $A = 4.0 \times 10^{-19}$ Pa^{-4} s^{-1}; $n = 4.0$; and $Q = 60$ kJ mol^{-1}. R is the gas constant (8.314 J mol^{-1} K^{-1}).

When the differential stress associated with ice ductile flow is set equal to the differential stress describing the brittle strength of ice, the T_{BDT} for ice is determined,

$$T_{BDT} = \left(\frac{Q}{nR} \right) \ln\left[(\sigma_1 - \sigma_3) \left(\frac{x_H A}{u d^p} \right)^{-n} \right]^{-1}. \quad (7)$$

Equations (1) and (7) can be solved by successive approximation to find self-consistent values of T_{BDT} and u.

The active lifetime of a band is

$$\tau = \frac{L}{u}, \quad (8)$$

where L is the band half-width.

We assume that vertical tension fractures in the band's hummocky zone will transition to normal faults when ice originally emplaced along the band axis cools and thickens sufficiently to permit shear failure. From Mohr–Coulomb theory, this occurs when lithostatic stress at the brittle ductile transition exceeds about 3 times the tensile strength T_0 of the ice,

$$3T_0 = \rho g (y_{BDT}) \quad (9)$$

(e.g., Suppe, 1985, p. 192). As discussed below, this tensile strength relationship is used to constrain driving stress mechanism most likely responsible for band spreading on Europa.

An assumed x_B/y_{BDT} for fault blocks fixes the depth to the BDT isotherm at a given horizontal distance from the central trough, most notably the width of the hummocky zone. Values for x_B/y_{BDT} in the range 1/10 to 1/2 are considered reasonable by analogy to terrestrial fault block dimensions (Mann et al., 1983; Mandl, 1988, p. 55). Controls

on the aspect ratio of fault blocks are not well understood (Mandl, 1988, p. 68), and fault blocks on Europa may have different aspect ratios than those observed in rock on Earth. As the x_B/y_{BDT} ratio increases, the inferred T_{BDT} increases as well. An upper limit of 1/2 for fault block dimensions is obtained from the T_{BDT} which corresponds to an upper limit $T_{BDT} = 190$ K (Nimmo and Manga, 2002).

3. Model results

Fig. 4 displays the half-spreading rates and brittle–ductile transition depths obtained by applying the MOR model described in Section 2.3 to the axisymmetric ridged band Yelland Linea. As summarized in Table 2, model results for Yelland and Ino Lineae are very similar in every case (as defined by ice rheology, coefficient of internal friction, and grain size), because their hummocky zone widths and fault block widths are similar.

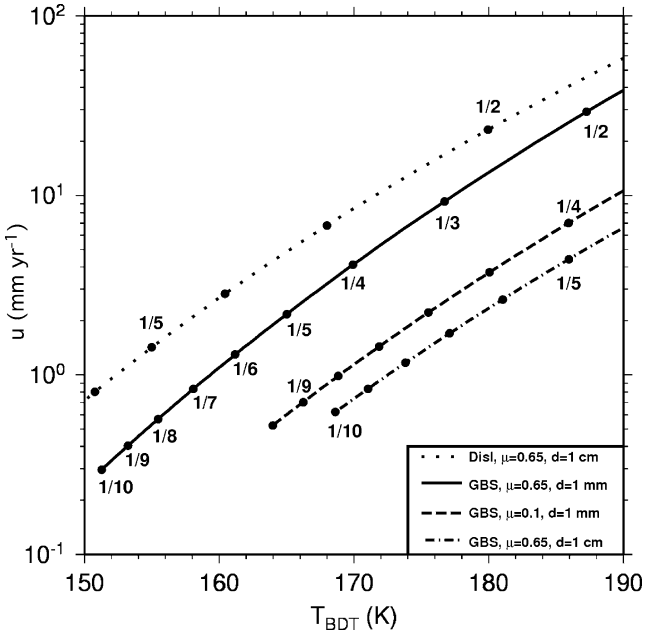

Fig. 4. Half-spreading rate (u) as a function of brittle–ductile transition temperature (T_{BDT}) for Yelland Linea. Ticks of fault block width-to-depth ratio (x_B/y_{BDT}) are labeled: for smaller assumed x_B/y_{BDT} ratios, lower BDT temperatures and slower opening rates are inferred. The nominal case (sold curve) is for a grain boundary sliding (GBS) ice rheology, with coefficient of friction $\mu = 0.65$ and grain size $d = 1$ mm. For GBS, assumptions of a smaller coefficient of friction (dashed curve: $\mu = 0.1$) or a larger grain size (dot-dashed curve: $d = 1$ cm) imply lesser opening rates. A dislocation creep ice rheology (dotted line: $\mu = 0.65$, $d = 1$ cm) predicts larger spreading rates and larger x_B/y_{BDT} ratios.

In our nominal case we use the GBS rheology for ice, a coefficient of internal friction $\mu = 0.65$, and an ice grain size $d = 1$ mm. For a x_B/y_{BDT} range 1/2–1/10, the band characteristics imply half-spreading rates 0.2–40 mm yr^{-1}, corresponding strain rates 8×10^{-15}–1×10^{-12} s^{-1}, active lifetimes 0.1–30 Myr, and an estimated range of tensile strength of ice at the time of fault formation 0.4–2.0 MPa. Results are reported independently for the two bands in Table 2.

The rheology of Europa's ice shell is not well constrained, so to test the sensitivity of this model to ice rheology, we consider how an assumption of dislocation creep rheology might change the results. Dislocation creep rheology is only valid for grain sizes of 1 cm and greater. Results show a significant difference from the GBS case for a grain size of 1 cm, extending the range of spreading rates and strain rates to nearly twice the upper limit for GBS. The active lifetimes for dislocation creep are approximately an order of magnitude less than lifetimes estimated for GBS creep, and predicted tensile strengths are smaller (Table 2).

The values of spreading rate are not strongly dependent on μ, but as the coefficient of friction increases, the variation in spreading rate as a function of width to depth ratio decreases. Changing the assumed ice grain size (for $\mu = 0.65$) shows that the range of inferred spreading rates is somewhat smaller for $d = 1$ cm than for $d = 1$ mm.

As a band forms, warm ice from Europa's deep shell is expected to flow toward the hummocky zone and be emplaced in the center of the band, potentially driving uplift of the band relative to the surrounding terrain (cf. Nimmo et al., 2003). The time scale for inflow of warm ice is $y_{BDT}/u \sim 10^5$ yr, which is similar to predictions of the active lifetime of the bands, confirming that warm ice is able to flow into an opening band.

The simple mid-ocean ridge cooling model of Turcotte and Schubert (2002) considers heat flow by conduction only, and it assumes that the thickness of the lithosphere goes to zero at the spreading axis. If vertical flow of ice were considered in the model, warm upwelling ice would cool as it reached the surface, forming a thin crust along the axis of an opening band. If the thickness of the chilled crust along the

Table 2
Model results for Yelland and Ino Lineae

	GBS ($\mu = 0.65$, $d = 1$ mm)		GBS ($\mu = 0.1$, $d = 1$ mm)		GBS ($\mu = 0.65$, $d = 1$ cm)		Dislocation creep ($\mu = 0.65$, $d = 1$ cm)	
	Yelland	Ino	Yelland	Ino	Yelland	Ino	Yelland	Ino
u (mm yr^{-1})	0.3–40	0.2–40	0.5–10	0.4–10	0.6–7	0.5–7	0.7–70	0.7–60
$\dot{\varepsilon}$ (s^{-1}) ($\times 10^{-12}$)	0.01–1	0.01–1	0.02–0.4	0.01–0.4	0.02–0.2	0.02–0.3	0.02–2	0.03–2
τ (Myr)	0.1–20	0.2–30	0.4–9	0.7–20	0.6–7	1–20	0.07–6	0.1–10
T_0 (MPa)	0.4–2	0.4–2	0.7–2	0.7–2	0.8–2	0.8–2	0.3–1	0.3–1
x_H/y_{BDT}	1/2–1/10	1/2–1/9	1/4–1/10	1/4–1/10	1/5–1/10	1/4–1/10	1/2–1/6	1/2–1/5

Table 3
Terrestrial parameters and model results

	Wet diabase ($\mu = 0.65$, $d = 1$ mm)
x_H (km)	5.0
x_B (km)	0.73
u (mm yr^{-1})	4.7–76
$\dot{\varepsilon}$ (s^{-1}) ($\times 10^{-12}$)	0.030–0.48
T_{BDT} (K)	770–920
T_0 (MPa)	16–47
x_H/y_{BDT}	1/2–1/6

band axis were comparable to the thickness of the brittle ice far from the ridge, a simple conductive cooling model would not accurately describe the behavior of the bands on Europa. We estimate the thickness of the crust at the center of the ridge by balancing cooling by thermal diffusion with advective heat transport. If the surface of the opening band is held constant at T_S, and warm ice moves upward at a rate equal to the spreading velocity, the crust is ∼10s to 100s m thick along the spreading axis. This is much smaller than the depth to the BDT in our model calculations, indicating that a simple conductive model reasonably approximates the behavior of bands on Europa.

Typical terrestrial spreading rates are reproduced by our model for a rheology relevant to mid-ocean ridges on Earth (Table 3). To characterize a terrestrial mid-ocean ridge, we use parameters for a wet diabase: $A = 10^{-3.7}$ MPa$^{-3.4}$ s^{-1}; $p = 0$; $n = 3.4$; and $Q = 260$ kJ mol^{-1} (Brace and Kohlstedt, 1980). Here we adopt $T_S = 273$ K, $T_D = 1500$ K, $\rho = 3300$ kg m^{-3}, $\mu = 0.65$, $d = 1$ mm, $g = 9.8$ m s^{-2}, and $\kappa = 1 \times 10^{-6}$ m^2 s^{-1}. For $T_{BDT} = 870$ K as expected in the vicinity of a terrestrial mid-ocean ridge, we find obtain $u = 40$ mm yr^{-1}, $\dot{\varepsilon} = 2 \times 10^{-13}$ s^{-1}, $y_{BDT} \sim 1/3$, and $T_0 = 20$ MPa. It is somewhat surprising that this simple works so well for the terrestrial case, considering the actual complexity of MOR processes on Earth. These results provide additional confidence in application of this model to Europa.

4. Discussion

The spreading and strain rates inferred for europan bands (Table 2) are similar to MOR spreading rates and continental rifting strain rates terrestrial rates (e.g., Turcotte and Schubert, 2002, p. 326). Moreover, derived band strain rates are consistent with a theoretical study of europan tectonics that predicts band-like rifting for ice shell thicknesses >10 km at $\dot{\varepsilon} > 10^{-14}$ s^{-1} (Nimmo, 2004). The estimated range for the tensile strength of Europa's ice (0.4–2 MPa) is similar to the typical strength (0.5 MPa) of naturally occurring terrestrial ice (Weeks and Assur, 1968; Vaudrey, 1977), to laboratory estimates (∼1 MPa) for polycrystalline ice (e.g., Petrenko and Whitworth, 1999, p. 206), and to values (0.2–0.5 MPa) independently inferred for Europa's ice by Nimmo (2004).

The nominal range of 0.4–2 MPa for the tensile strength of ice for both bands implies a driving stress mechanism that can produce relatively large stress magnitudes. Thermal buoyancy produces small stresses of ∼0.001–0.01 MPa (Tobie et al., 2003) which would be unable to drive band opening. Diurnal stresses (∼0.1 MPa) are also too small. Nonsynchronous rotation of the icy shell can produce sufficient stress over ∼4° to 20° of shell rotation (Leith and McKinnon, 1996) to fracture ice of the strength range derived here. Polar wander has been suggested as a mechanism for opening bands in Argadnel Regio (Leith and McKinnon, 1996), but stresses are just ∼30% those of nonsynchronous rotation. Thus, nonsynchronous rotation (plausibly in combination with polar wander) is implicated as the probable dominant driving mechanism for opening of Yelland and Ino Lineae, rather than thermal buoyancy or diurnal stresses.

It has been suggested that bands in Argadnel Regio formed nearly simultaneously (Schenk and McKinnon, 1989), in a region of near-isotropic tension (Pieri, 1981) or perhaps near-isotropic compression (Schulson, 2002). Nonsynchronous rotation produces near-isotropic "equatorial compressional zones" (ECZs) alternating with "equatorial tensile zones" (ETZs), each of which spans ∼90° in longitude across Europa's tropics (Helfenstein and Parmentier, 1985; McEwen, 1986; Leith and McKinnon, 1996; Spaun et al., 2003). Yelland and Ino Lineae are currently in the eastern portion of an ETZ, and nonsynchronous rotation implies that Europa's surface rotates slowly eastward relative to these stress regimes.

Development of a wedge-shaped band by isotropic compression and shear motion implies that the long-axis of the band formed ∼30° from the principal compressive stress direction (Schulson, 2002; Spaun et al., 2003). Fig. 5 illustrates that under this assumption, Yelland's N-NW orientation would imply back-rotation through ∼150° of longitude to the ECZ location in which it could have formed most recently. Ino Linea, which is cross-cut by Yelland and is therefore older, would then have to be back-rotated through ∼260° of longitude for its E-NE orientation to match ECZ stress orientations. This implies at least ∼260° of nonsynchronous rotation (or multiples of 180° more) to account for formation of Ino Linea and then Yelland Linea each in compressional zones. Alternatively, if these bands developed in equatorial tensile zones (Fig. 5), with the least compressive stress (tensile in this case) oriented perpendicular to the bands' long axes, then Yelland's N-NW orientation fits the current ETZ stresses. Ino's E-NE orientation would require ∼50° of back-rotation to align Ino perpendicular to ETZ stresses. Overall, formation of these bands in an ETZ requires a minimum of just ∼50° of nonsynchronous rotation.

In one small portion of Argadnel Regio imaged by Galileo, approximately 60% of the terrain is recognized as having band-like morphology (Prockter et al., 2002), suggesting that band formation has been a significant contribution to Europa's resurfacing. As a consistency check of our band opening rate results, we consider the time scale

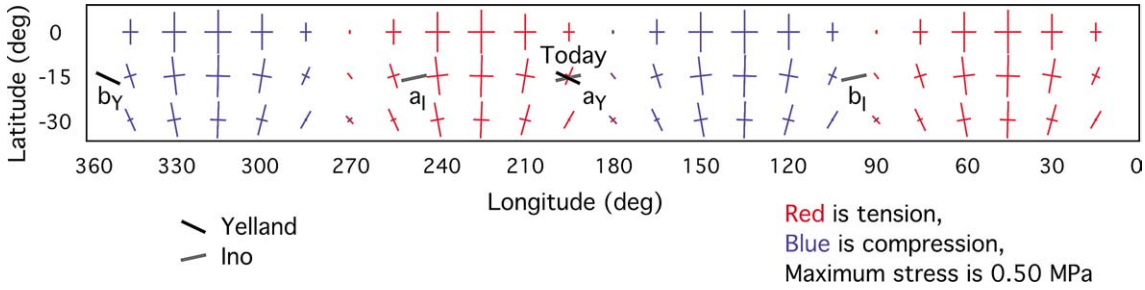

Fig. 5. The younger Yelland Linea (dark line) and older Ino Linea (gray line) intersect near 16° S, 196° W at their present positions. Here they are shown overlain on the surface stresses from 5° of nonsynchronous rotation of Europa's ice shell. If these bands formed in equatorial tensile zones, Yelland could have formed close to its present location (a_Y) relative to the nonsynchronous rotation stress pattern, and older Ino could have formed ∼50° westward (a_I) relative to the stress field (or any 180° multiples thereof). If the bands instead formed in equatorial compressional zones, Yelland could have formed if the ice shell has since rotated by ∼150° (b_Y), and Ino if the shell has since rotated by ∼260° (b_I), relative to the nonsynchronous rotation stress field (or 180° multiples thereof).

required to resurface Argadnel Regio with bands. We take the region's total area as $\sim 1 \times 10^6$ km^2, a nominal band length as ∼100 km, and a representative half-spreading rate as 10 mm yr^{-1}. If ∼10 such bands form near-simultaneously with no overlap, then resurfacing of Argadnel Regio can occur in ∼10 Myr. This resurfacing rate is broadly consistent with the ∼60 Myr surface age of Europa (Zahnle et al., 2003), suggesting that a 10 mm yr^{-1} band opening rate is in accord with the density of bands in Argadnel Regio.

5. Conclusions

A terrestrial mid-ocean-ridge spreading model has been applied to band spreading on Europa to infer spreading rates and the sub-surface thermal structure in the vicinity of bands. The model assumes that cooling of emplaced material occurs with time, such that the brittle layer becomes thick enough to fault at some lateral distance from the band axis, defining the lateral extent of a band's hummocky zone. The brittle layer is assumed to be underlain by a warm, ductile layer of ice, which moves upward buoyantly as extension is concentrated along the weak band axis.

For an average fault spacing and assumed width-to-depth ratio of fault blocks, the cooling model, coupled with an expression of the brittle–ductile transition depth as constrained by a lithospheric strength envelope, provides self-consistent values for the brittle–ductile transition temperature and the band half-spreading rate. The strain rate, active lifetime, and tensile strength of ice are also constrained.

Implied half-spreading rates in a grain-boundary sliding regime are in the range of 0.2–40 mm yr^{-1} for Yelland and Ino Lineae. Corresponding strain rates for nominal parameter assumptions range from 8×10^{-15} to 1×10^{-12} s^{-1}, and nominal active lifetimes range from 0.1 to 30 Myr for Yelland and Ino Lineae. The inferred tensile strength of band ice is to 0.4–2 MPa, implying that nonsynchronous rotation (plausibly in combination with polar wander) is the probable stress mechanism of band opening, while thermal buoyancy or diurnal stresses are insufficient. If Yelland and Ino Lineae each formed within an equatorial compressional zone (ECZ), this suggests that at least ∼260° of icy shell nonsynchronous rotation has occurred; in contrast, formation of each band within an equatorial tensional zone (ETZ) requires that the icy shell has experienced a minimum of just ∼50° degrees of nonsynchronous rotation.

The validity of this scenario for formation of Europa's bands can be tested with future spacecraft data. Ice-penetrating radar can potentially identify subsurface melt zones to constrain the sub-surface thermal structure, and may be able to map faults within the band material. Measurements of heat flow in the vicinity of bands could be used to constrain their opening rates.

Acknowledgments

We thank Francis Nimmo and Michael Manga for very helpful reviews, and Roger Buck for valuable discussions. Support for this work is provided by NASA Planetary Geology and Geophysics Grant NNG04GJ19G.

References

Beeman, M., Durham, W.B., Kirby, S.H., 1988. Friction of ice. J. Geophys. Res. 93, 7625–7633.

Brace, W.F., Kohlstedt, D.L., 1980. Limits on lithospheric stress imposed by laboratory experiments. J. Geophys. Res. 85, 6248–6252.

Figueredo, P.H., Greeley, R., 2000. Geologic mapping of the northern leading hemisphere of Europa from Galileo solid-state imaging data. J. Geophys. Res. 105, 22629–22646.

Figueredo, P.H., Greeley, R., 2004. Resurfacing history of Europa from pole-to-pole geological mapping. Icarus 167, 287–312.

Goldsby, D.L., Kohlstedt, D.L., 2001. Superplastic deformation of ice: Experimental observations. J. Geophys. Res. 106, 11017–11030.

Greeley, R., Chyba, C.F., Head, J.W., McCord, T.B., McKinnon, W.B., Pappalardo, R.T., Figueredo, P., 2004. Geology of Europa. In: Bagenal, F., Dowling, T.E., McKinnon, W.B. (Eds.), Jupiter: The Planet, Satellites, and Magnetosphere. Cambridge Univ. Press, Cambridge, UK, pp. 329–362.

Greenberg, R., Geissler, P.E., Hoppa, G.V., Tufts, B.R., Durda, D.D., Pappalardo, R.T., Head, J.W., Greeley, R., Sullivan, R., Carr, M.H., 1998.

Tectonic processes on Europa: Tidal stresses, mechanical response, and visible features. Icarus 135, 64–78.
Gudmundsson, A., 1987. Geometry, formation and development of tectonic fractures on the Reykjanes Peninsula, southwest Iceland. Tectonophysics 139, 295–308.
Head, J.W., Pappalardo, R.T., Sullivan, R., 1999. Europa: Morphological characteristics of ridges and triple bands from Galileo data (E4 and E6) and assessment of a linear diapirism model. J. Geophys. Res. 104, 24223–24236.
Helfenstein, P., Parmentier, E.M., 1985. Patterns of fracture and tidal stresses due to nonsynchronous rotation: Implications for fracturing on Europa. Icarus 61, 175–184.
Hoppa, G.V., Tufts, B.R., Greenberg, R., Geissler, P.E., 1999. Strike-slip faults on Europa: Global shear patterns driven by tidal stress. Icarus 141, 287–298.
Jaeger, J.C., Cook, N.G.W., 1979. Fundamentals of Rock Mechanics, third ed. Chapman and Hall, London, UK, 96 pp.
Kennedy, F.E., Schulson, E.M., Jones, D.E., 2000. The friction of ice on ice at low sliding velocities. Philos. Mag. A 80, 1093–1110.
Leith, A.C., McKinnon, W.B., 1996. Is there evidence for polar wander on Europa? Icarus 120, 387–398.
Mandl, G., 1988. Mechanics of Tectonic Faulting: Models and Basic Concepts. Elsevier, New York, pp. 55, 68.
Mann, P., Hempton, M.R., Bradley, D.C., Burke, K., 1983. Development of pull-apart basins. J. Geol. 91, 529–554.
McEwen, A.S., 1986. Tidal reorientation and the fracturing of Jupiter's moon Europa. Nature 321, 49–51.
Nimmo, F., 2004. Dynamics of rifting and modes of extension on icy satellites. J. Geophys. Res. 109, E01003, 10.1029/2003JE002168.
Nimmo, F., Manga, M., 2002. Causes, characteristics and consequences of convective diapirism on Europa. Geophys. Res. Lett. 29, 10.1029/2002GL016660.
Nimmo, F., Pappalardo, R.T., Giese, B., 2003. On the origins of band topography, Europa. Icarus 166, 21–32.
Petrenko, V.F., Whitworth, R.W., 1999. Physics of Ice. Oxford Univ. Press, Oxford, UK, 206 pp.
Pieri, D.C., 1981. Lineament and polygon patterns on Europa. Nature 289, 17–21.
Prockter, L.M., Head, J.W., Pappalardo, R.T., Sullivan, R., Clifton, A.E., Giese, B., Wagner, R., Neukam, G., 2002. Morphology of europan bands at high resolution: A mid-ocean ridge-type rift mechanism. J. Geophys. Res. 107, 10.1029/2000JE001458.
Schenk, P.M., McKinnon, W.B., 1989. Fault offsets and lateral crustal movement on Europa: Evidence for a mobile ice shell. Icarus 79, 75–100.
Schulson, E.M., 2002. On the origin of a wedge crack within the icy crust of Europa. J. Geophys. Res. 107, 10.1029/2001JE001586.
Spaun, N.A., Pappalardo, R.T., Head, J.W., 2003. Evidence for shear failure in forming near-equatorial lineae on Europa. J. Geophys. Res. 108, 10.1029/2001JE001499.
Sullivan, R., Greeley, R., Homan, K., Klemaszewski, J., Belton, M., Carr, M., Chapman, C., Tufts, B.R., Head, J.W., Pappalardo, R.T., Moore, J., Thomas, P., the Galileo Imaging Team, 1998. Episodic plate separation and fracture infill on the surface of Europa. Nature 391, 371–372.
Suppe, J., 1985. Principles of Structural Geology. Prentice–Hall, Englewood Cliffs, NJ.
Tobie, G., Choblet, G., Sotin, C., 2003. Tidally heated convection: Constraints on Europa's ice shell thickness. J. Geophys. Res. 108, 10.1029/2003JE002099.
Turcotte, D.L., Schubert, G., 2002. Geodynamics, second ed. Cambridge Univ. Press, Cambridge, UK, pp. 153–159, 326.
Vaudrey, K.D., 1977. Ice engineering study of related properties of floating sea-ice sheets and summary of elastic and viscoelastic analyses. Technical Report TR-860, Civil Engineering Laboratory, Alexandria.
Weeks, W.F., Assur, A., 1968. The mechanical properties of sea ice. In: Ice Pressures Against Structures. Proceedings of a Conference held at Laval University, Quebec, 10–11 November 1966. Assoc. Committee on Geotech. Res. of the Natl. Res. Council of Canada, Ottawa, pp. 25–78. Tech. Memo. No. 92.
Zahnle, K.L., Schenk, P., Levison, H.F., Dones, L., 2003. Cratering rates in the outer Solar System. Icarus 163, 236–289.